

Simulated multi-component CuZr(Al) metallic glasses akin to experiments

Rene Alvarez-Donado¹, Silvia Bonfanti¹, Mikko Alava^{1,2}

¹ *NOMATEN Centre of Excellence, National Center for Nuclear Research,
ul. A. Soltana 7, 05-400 Swierk/Otwock, Poland*

² *Aalto University, Department of Applied Physics, PO Box 11000, 00076 Aalto, Espoo, Finland*

We study a three-component CuZrAl metallic glass system by means of a combined Monte Carlo and Molecular Dynamics simulations scheme. This hybrid method allows us to generate equilibrated samples at temperatures below the conventional glass transition for the first time, achieving a more stable glassy regime. By using a realistic potential for the interactions of metallic species, we explore the kinetics, thermodynamics, and rheology of a CuZrAl glass, and then compare these findings with those of the ubiquitous CuZr. Remarkably, the resulting sheared glassy configurations show an abrupt stress drop corresponding to the shear band, akin to experimental observations. Our results pave the way for theoretical studies of complex metallic glasses and offer comparisons with experiments.

Metallic glasses (MGs) are an important class of materials constituted by an amorphous atomic structure, which forms when the high-temperature metallic liquid is rapidly cooling down to room temperature [1–3]. The unique disordered structure thereby formed is the key to many outstanding properties, such as unprecedented mechanical features, including high strength and high elastic limit. Hence, MGs have great potential to outperform conventional materials for various technological and industrial applications [2, 4, 5]. Nevertheless, the major limitation that prevents their use on a large scale, is the difficulty to avoid the crystallization of the samples during the cooling process [6]. Recent advancement in synthesis techniques has come from a method different from conventional cooling: vapor deposition. This technique allows the production of MGs with enhanced stability, known as ultrastable metallic glasses (UMGs) [7–11]. A resultant shift in the glass transition temperature, indicative of this enhanced stability, has been observed in various UMGs such as for Cu₄₆Zr₄₆Al₈ MG in Ref. [9]. These glasses are thought to be equivalent to conventionally liquid quenched MGs that have undergone aging for thousands of years [12]. This trend was initially discovered by Ediger and co-workers but in the class of organic glasses [13]. In general, ultrastable glasses are characterized by extraordinary thermodynamic and kinetic stability and exceptional mechanical properties [13–16]

The molecular mechanisms underlying the glass-forming ability (GFA), shift of glass transition temperature, and formation of enhanced stable states in MGs are far from being understood, a challenge that also characterizes the broad spectrum of glasses [17, 18]. Molecular simulations have been fundamental to investigate the properties of glasses from the microscopic point of view [19, 20]. However, simulations suffer from unrealistic high-cooling rates ($\sim [10 - 1000]$ K/ns), resulting in computer-generated metallic glasses with properties that differ significantly from those observed in experiments [21–25]. Here, we solve this gap by obtaining *in silico* samples of realistic CuZr-based ultrastable

MGs similar to experiments, using an efficient hybrid Molecular Dynamics and Monte Carlo (MD+MC) simulation approach. Our study focus on two-component Cu₅₀Zr₅₀ MGs as a starting point, and ternary component Cu₄₆Zr₄₆Al₈ MGs, both known for their exceptional GFA, outstanding mechanical properties and significant potential in engineering applications [9, 26–29].

Recently, the limitation of timescale of standard simulations has been overcome through the development of a very efficient method, called Swap Monte Carlo (SMC) [30–32]. Here the equilibration time increases less rapidly than the relaxation time τ_α as the temperature decreases [33, 34], allowing for the computation of the equilibrium configurational entropy below the experimental T_g [35–37]. The SMC algorithm has seemed to be the sole means to investigate the properties of ultrastable glasses *in silico*. Despite the accelerated dynamics facilitated by swap moves, the crystallization effects commonly observed in conventional simulations continue to occur in SMC, but can be resolved by enforcing a degree of polydispersity, which effectively prevents crystallization and enables the generation of deeply cooled equilibrium liquid configurations, even at temperatures below the glass transition T_g , comparable with experiments. So far SMC has been applied only to a simplified model of metallic glass, a ternary mixture Lennard-Jones, that does not consider the specific nature of the constituents [38], therefore limiting our knowledge of the chemical composition landscape for MGs.

An intriguing solution to accelerate the dynamics sampling in the chemical configuration space [39] comes from the field of multicomponent crystalline alloys and combines MC methods, MD, and realistic short range potential, e.g. Embedded Atom Method (EAM) [40]. Only very recently, this technique has been applied in glasses to obtain more stable realistic samples of binary CuZr MG in computer simulations [41], where it was shown that shear transformation zones are limited to small clusters of particles. Here, we demonstrate how this approach is suitable for tackling various concentrations of different

species and that it is applicable to produce more stable realistic samples of *multicomponent* MGs *in silico*. We introduce for the first time equilibrium configurations of ternary metallic MGs, specifically $\text{Cu}_{46}\text{Zr}_{46}\text{Al}_8$, approaching experiments. We examine their thermodynamic and more stable states and compare the mechanical properties. Our work presents a first example of generating computationally realistic models for any type of metallic glass consisting of several atomic species.

Simulation methods — The interatomic interactions are simulated through an Embedded Atom Method (EAM) as developed by [27]. For thermodynamics and kinetics, we performed simulations consisting of $N=1500$ atoms in a cubic box with periodic boundary conditions in three dimensions. Our simulations are performed with LAMMPS [42], using a time step $\Delta t=1$ fs. The glass state is obtained through quenching in the isobaric-isothermal ensemble (NpT) from the liquid at 2000 K to 300 K using a cooling rate $\kappa=10^{12}$ K/s. We save configurations every 50 K during the cooling process for further analysis. The cooling process is performed by integrating the Nosé-Hoover equations with damping parameters $\tau_T=2$ fs and $\tau_p=5$ ps for the thermostat and barostat. All results are obtained keeping the external pressure $p=0$.

Hybrid Molecular Dynamics-Monte Carlo (MD+MC) algorithm — In order to generate glasses that attempt to emulate the mechanical behavior observed in experiments, we employ a hybrid Molecular Dynamics-Monte Carlo (MD+MC) scheme under the variance-constrained semi-grand canonical ensemble (VC-SGC) [39]. Differently from traditional SMC, this VC-SGC MC scheme allows exploring the configurational degrees of freedom by randomly selecting an atom and attempting to change its type, while also calculating the corresponding energy and *concentration* changes. It allows to target specific concentration ranges while maintaining fixed total number of particles and the volume. Acceptance of these transmutations follows the Metropolis criterion, ensuring the preservation of detailed balance. On the other hand, the relaxation processes are accounted for by the MD integration steps. To maintain the desired concentration within the system [39], we set the variance parameter $\kappa=10^3$. Furthermore, we evaluate the differences in chemical potential relative to Zr using hybrid MD+MC simulations under the semi-grand canonical ensemble at a temperature of 2000 K. The specific set of parameters that minimize the composition errors in relation to the desired concentration can be found in the Appendix.

Quenching Protocol — The quenching is performed starting from molten metals at high temperature well above the melting point using a fixed cooling rate of 10^{12} K/s at fixed pressure. For the MD+MC scheme, every 20 MD steps, a MC cycle consisting of $N/4$ attempts is performed. For a comparison between different cooling rates with MD and MD+MC, see Appendix.

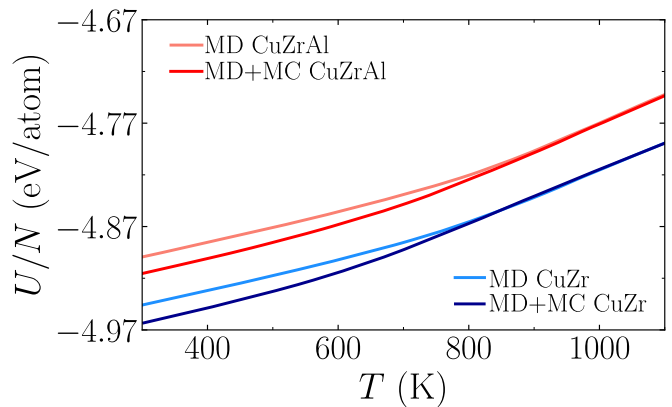


FIG. 1. Thermal evolution of the potential energy per atom of the binary $\text{Cu}_{50}\text{Zr}_{50}$ and the ternary $\text{Cu}_{46}\text{Zr}_{46}\text{Al}_8$ MGs with a cooling rate of 10^{12} K/s using both a pure MD and a hybrid MD+MC algorithm (red lines). At high temperatures, both methods exhibit similar results. However, as the temperature decreases, the behavior diverges significantly. The MC+MD method remains in equilibrium for lower temperatures compared to the pure MD approach.

Results — First, we compare the thermal evolution of the potential energy per particle between a conventional MD simulation and our MD+MC scheme for the two MG systems. Figure 1 reports the potential energy per atom (U/N) as a function of the temperature T during quenching, obtained by averaging over 5 independent simulations. Notably, the hybrid algorithm allows us to quench the liquid at lower temperatures, increasing the chance of reaching more stable configurations and properties similar to those observed in experiments. Note that both methods, MD and MC+MD, exhibit the same trend at high temperatures, as expected.

After the quenching we evaluate the relaxation time of the two different dynamics: conventional MD and MC+MD, for the ternary CuZrAl system. For each temperature we switch from NpT to NVT ensemble and run equilibration runs to compute the self-part of the intermediate scattering function [32]. For the case of MC+MD we employ the VC-SGC method as described above. The relaxation time, τ_α , defined as the value at which the intermediate scattering function is equal to $1/e$, is reported in Fig. 2 for the standard MD (circles) and MC+MD dynamics (squares). The speedup of the dynamics given by our MD+MC scheme is shown as about two orders of magnitude at the lowest temperature.

It is well known that the GFA of CuZr MG improves when a small percentage of Al is included [7]. In a previous study of the same MG [43], we estimated T_g^{MD} to be 623 K and 713 K for $\text{Cu}_{50}\text{Zr}_{50}$ and $\text{Cu}_{46}\text{Zr}_{46}\text{Al}_8$, respectively. By following a similar protocol, we observe the same trend in the MD+MC algorithm, indicating

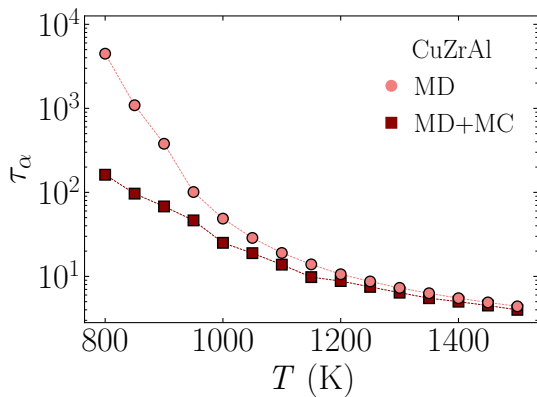


FIG. 2. Comparison of relaxation time τ_α for standard MD simulations and hybrid MD+MC with VC-SGC method for the ternary CuZrAl MG. The speedup offered by the MD+MC dynamics is evident.

that the method mimics the melt-quench procedure but provides equilibrium configurations for temperatures below the conventional T_g , meaning that it creates more stable glasses. Throughout the quenching process, in both pure MD and MD+MC, we carefully analyzed the structure and found no evidence of crystallization in the alloys.

Thermodynamics — Once we successfully create glasses approaching experimental conditions, our focus shifts to exploring their thermodynamic properties. To being with, we determine the configurational entropy of the glass formed by MD+MC by the formula $S_{conf} = S_{tot} - S_{vib}$, where S_{tot} represents the total entropy and S_{vib} stands for the vibrational contribution. We obtain both entropies using the reversible scaling (RS) method [44], with the Uhlenbeck-Ford potential and the Einstein crystal serving as reference systems, respectively [45–47] (see Supplementary Information). Figure 3 displays the configurational entropy (S_{conf}) plotted against temperature for both the binary $\text{Cu}_{50}\text{Zr}_{50}$ and ternary $\text{Cu}_{46}\text{Zr}_{46}\text{Al}_8$ alloys. As anticipated, S_{conf} decreases with decreasing temperature until it freezes in at lower temperatures due to the glass transition. The measured residual entropy values, representing the constant S_{conf} value at the occurrence of the glass transition, were 0.049 and 0.035 J/mol-K for $\text{Cu}_{50}\text{Zr}_{50}$ and $\text{Cu}_{46}\text{Zr}_{46}\text{Al}_8$, respectively. Note in particular that the S_{conf} of $\text{Cu}_{46}\text{Zr}_{46}\text{Al}_8$ are lower than the binary alloy, the reason for that is because the ternary alloy possesses a high GFA allowing to reach deeper values before the freeze-in at T_g (which is higher). The reported value of S_{conf} in the $\text{Cu}_{50}\text{Zr}_{50}$ alloy is just a 20% from the one reported *in situ* by Smith *et al.* [48]. We are dealing with glass configurations with glass transition temperatures lower than the one obtained in conventional glasses, thus it is expected to have a lower value of the residual

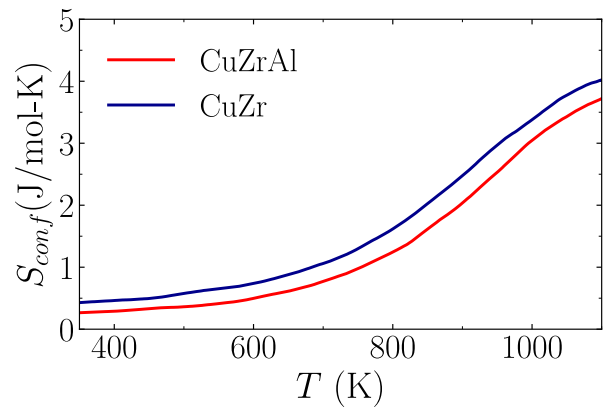


FIG. 3. Configurational entropy as a function of temperature obtained through RS method for $\text{Cu}_{50}\text{Zr}_{50}$ (blue) and $\text{Cu}_{46}\text{Zr}_{46}\text{Al}_8$ (red).

entropy. A comparison with experiments for the ternary system is currently not available.

Following experiments on ultra stable MGs using vapor-deposition method, a common approach to studying their stability is by performing calorimetric measurements during a heating process. In Figure 4, we compare the behavior of glasses prepared using

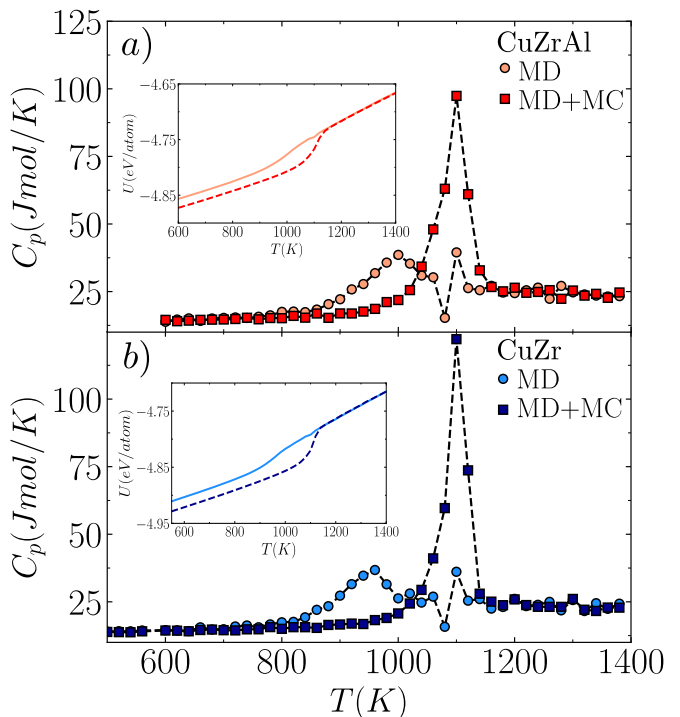


FIG. 4. Heat capacity as a function of temperature obtained through RS method for a) $\text{Cu}_{46}\text{Zr}_{46}\text{Al}_8$ and b) $\text{Cu}_{50}\text{Zr}_{50}$. The insets show the potential energy of the binary and ternary alloys, respectively, as a function of temperature during the heating process using MD (thin lines) and MD+MC (dashed lines).

conventional MD with those created using the MD+MC algorithm. We heat the glass at the same rate of 10^{12} K/s and save the configuration every 20 K. Then, we compute the heat capacity using its statistical definition: $(\langle E^2 \rangle - \langle E \rangle^2)/k_B T^2$, where E is the energy of the system, and k_B is the Boltzmann constant. The insets of Figures 4a) and 4b) with the potential energy of the binary and ternary alloys, respectively, illustrate as well via the difference of the two kinds of glasses as a function of temperature. Clearly, the devitrification process of the glass created through the hybrid MD+MC happens at a higher temperature, approximately 18% above T_g [15, 49, 50]. In vapor-deposited experiments [7], this temperature is called the “onset” temperature T_o , and it is generally between 6 to 10% above the conventional T_g , reflecting the much larger kinetic stability reached by this method. Since our MD+MC glass produces similar results, we can confirm that the $\text{Cu}_{46}\text{Zr}_{46}\text{Al}_8$ and $\text{Cu}_{50}\text{Zr}_{50}$ alloys produced by this method are more stable configurations.

Rheology — For mechanical tests we perform athermal quasistatic simulations [51] starting from configurations with $N=100000$ atoms, at $T=300$ K cooled down to 0 K, following the work of Ref. [52]. We shear the simulation box along the x direction by the amount $\delta\gamma$. We perform energy minimization after each strain step with the fast inertial relaxation engine (FIRE) [53] until the system reaches mechanical equilibrium, until a maximum force of $10^{-10}\text{eV}/\text{\AA}$ is reached.

Figure 5 (top) shows how the composition and the history influence the mechanical behavior. The addition of aluminum increases by a few percent the shear modulus [54], and to compare the glasses at peak stress we scale away the dependence of on the modulus. These are typical stress-strain curves, where after an initial elastic part we see the typical glass response: strain-softening close to the maximum, fluctuations, and a drop in stress before plastic flow. In particular, as in model glasses [41] we observe that the more stable glasses exhibit drastic stress drops which corresponds to the appearance of a system-spanning shear band (Inset). The well-prepared glasses do so at slightly larger strains than the basic ones, and in scaled units they are noticeably stronger, here about 20%. The final state of flow one finds may be summarized by the examples of the strain fields in the Fig. 5 (bottom), with the features associated with the post-yield shear bands depending on the nature of the stress-peak: for glasses with enhanced stability we find a well-defined shear band whereas for the reference glass the band is more diffuse [38].

Summary & Conclusions — In order to resolve the physics of glasses *in silico* - a big challenge due to the complexity of glasses and their history-dependence - novel ideas are needed. In this work, we show for the first time how a combination of Molecular Dynamics and

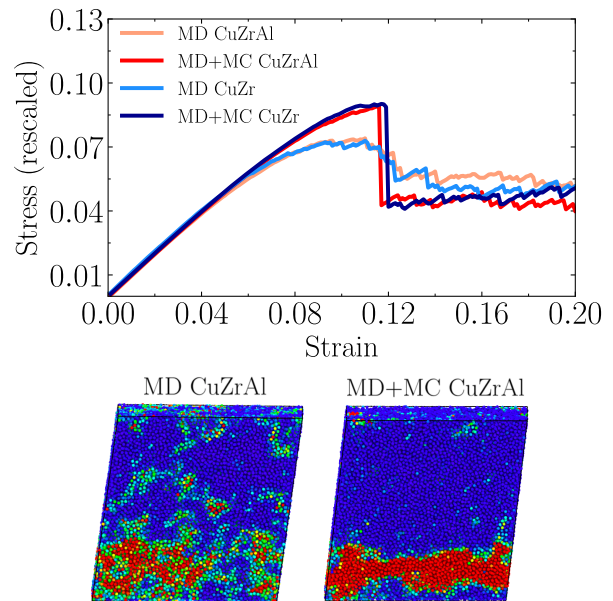


FIG. 5. Scaled shear-modulus stress-strain curves for MD and MD+MC schemes (upper panel). Strain inhomogeneity maps for a strain of 0.125 for the CuZrAl cases. The color bar indicates the non affine displacements from the unstrained configuration, from 0% (blue) to 20% (red).

Monte Carlo with VC-SGC method is able to tackle this issue for realistic multi-component MGs.

We present results that clearly show a convergence to the experimental observations as regards the thermodynamics of these systems, we also demonstrate, that such glasses have the ultrastable character, aligning them closely with vapor-deposited experimental counterparts. Finally, this fact is seen to make a difference in the mechanical properties. The next steps to follow are a through exploration of the relaxation times the MC+MD approach leads to and the subsequent changes in the yielding.

In conclusion, our results provide a substantial contribution to the field of glass physics, particularly with regard to multicomponent MGs with more than two component species [55, 56]. Using advanced simulations to obtain ultrastable glassy states, we provide an essential theoretical framework for further studies, shedding light on the underlying physical mechanisms governing the complex behaviors and properties of these amorphous materials. Our work prompts further theoretical investigations aimed at probing the microscopic mechanisms of complex MGs at a fundamental level, such as their relaxation dynamics and facilitation [57]. The methodologies employed in this work not only serve as a benchmark for experimental comparison but also suggest new avenues for optimizing the structure of MGs via cooling and processing techniques, for a range of applications.

Acknowledgements: We gratefully thank Anshul Par-

mar and Misaki Ozawa for fruitful discussions. Funding: RAD, SB, and MA are supported by the European Union Horizon 2020 research and innovation program under grant agreement no. 857470 and from the European Regional Development Fund via the Foundation for Polish Science International Research Agenda PLUS program grant No. MAB PLUS/2018/8.

APPENDIX

Setting VC-SGC parameters

In the variance-constrained semi-grand canonical (VC-SGC) ensemble[39], the system explores configurational degrees of freedom by randomly selecting an atom and attempting to change its type. The change in energy and concentration is then computed, and transmutations are accepted or rejected based on the Metropolis criterion, ensuring detailed balance and equilibrium sampling of the phase space. To determine the difference in chemical potential species ($\Delta\mu$), which fixes the desired composition and minimizes error, we conduct a series of semi-grand-canonical (SGC) simulations at a temperature of $T=2000$ K.

Figure 6 depicts the behavior of $\Delta\mu$ with regard to Zr for a) Cu and b) Al for a series of SGC simulations. The blue line is obtained expanding $\Delta\mu$ as a polynomial in concentration as follows:

$$\Delta\mu(X_{\text{Zr}}, p, T) = T \ln \left(\frac{X_{\text{Zr}}}{1 - X_{\text{Zr}}} \right) + \sum_{i=0}^n A_i X_{\text{Zr}}^i, \quad (1)$$

where X_{Zr} is the Zr composition and the coefficient A_i are fitting parameters.

By utilizing Eq (1), we can effectively determine the chemical potential at any desired composition. For both the binary $\text{Cu}_{50}\text{Zr}_{50}$ and ternary $\text{Cu}_{46}\text{Zr}_{46}\text{Al}_8$ alloys, the calculated chemical potential differences were $\Delta\mu_{\text{Zr-Cu}} = -2.69854$ eV, and $\Delta\mu_{\text{Zr-Cu}} = -2.90351$ eV, $\Delta\mu_{\text{Zr-Al}} = -0.55781$ eV, respectively. Once the composition is defined, we proceed with the hybrid MC+MD simulation under the VC-SGC ensemble. This combination of MD+MC efficiently allows us to create *in silico* glasses with properties similar to the ones obtained in experiments.

Cooling rate comparison

In Figure 7, we compare the thermalization efficiency of the hybrid MC+MD algorithm with conventional MD simulations. Starting from high temperatures well above the melting point, we rapidly cool the liquid using fixed cooling rates of 10^{14} , 10^{13} , and 10^{12} through MD simulation. With the hybrid MC+MD approach, we observe the same cooling rate-dependent trend at higher

temperatures. However, when employing the MC+MD algorithm, the liquid deviates from equilibrium at lower temperatures. The agreement among all the curves at high temperatures confirms the proper utilization of the MC+MD approach in our simulations.

Computing the configurational entropy

We have numerically calculated the entropy by means of the thermodynamic relation $S = (H - G)/T$, where H and G are the enthalpy and Gibbs free energy of the system, respectively. Since free energy is a thermal property [58] we are not able to compute it directly from conventional MD simulations. Thus, we have used a combination of the adiabatic switching (AS)[59, 60] and reversible scaling (RS)[61, 62] methods, which in principle allows the estimation of the free energy for a wide range of temperatures in a single simulation. We estimated the free energy (and the entropy) by carrying out the following steps:

- (i) The preparation of the initial state in which we want to calculate the free energy. This state is defined as:

$$\mathcal{H}_{\text{MEAM}}(\Gamma_\alpha) = \mathcal{T}(\Gamma_\alpha) + U_{\text{EAM}}(\Gamma_\alpha), \quad (2)$$

where $\mathcal{H}_{\text{MEAM}}$ is the Hamiltonian of the alloy described by EAM potential, \mathcal{T} and U_{EAM} are the kinetic and potential energy, respectively. Γ_α is a phase space vector with information of all momenta and positions as a function of time, and the subindex α holds to crystal (g) or liquid (l).

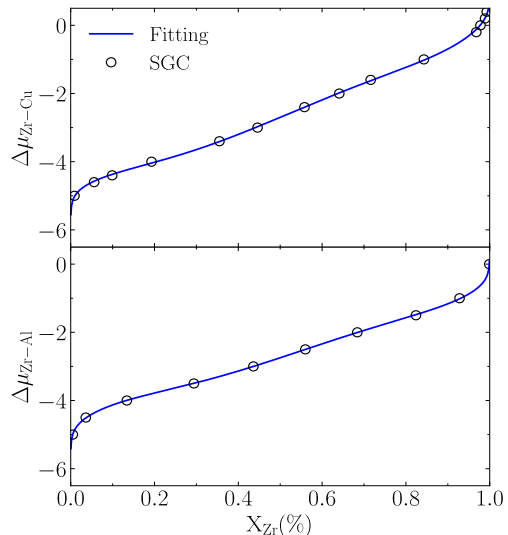


FIG. 6. Chemical potential as a function of the composition for a) Zr-Cu and b) Zr-Al from SGC simulations at $T=2000$ K. The blue solid line is a fitting obtained by Eq. 1.

- (ii) Once defined the initial state, we estimate its absolute free energy through AS method. The AS is a variation of the thermodynamic integration method[63] where the Hamiltonian of the initial state is coupled with a reference system whose free energy is known beforehand. However, the work done is obtained dynamically in one single simulation. Thus, the free energy is obtained by means of:

$$G_{\text{EAM}}^0 = G_{\text{Ref}}^\alpha + W_{\text{AS}}, \quad (3)$$

where G_{EAM}^0 is the free energy of the alloy in the initial state, G_{Ref}^α is the free energy of the reference system, and W_{AS} is the quasistatic work obtained through AS-method.

- (iii) Using the value of G_{EAM}^0 and the RS method we obtain the alloy-free energy for a wide range of temperatures. This method is based on writing the initial Hamiltonian in the parametric form[61]:

$$\mathcal{H}_{\text{EAM}}(\Gamma_\alpha, \zeta(t)) = \mathcal{T} + \zeta(t)U_{\text{EAM}}. \quad (4)$$

Here each value of ζ corresponds to a particular state of H_{EAM} in a particular temperature and we use \mathcal{T} and U_{EAM} instead of $\mathcal{T}(\Gamma_\alpha)$ and $U_{\text{EAM}}(\Gamma_\alpha)$ to simplify the notation. One can show that using Eq. (4) the free energy of the alloy at any temperature is given by the equation[44, 61]:

$$G_{\text{EAM}}(T) = \frac{G_{\text{EAM}}^0}{\zeta} + \frac{3}{2}nk_B T_0 \frac{\ln \zeta}{\zeta} + \frac{1}{\zeta} \int_0^{t_{\text{sim}}} dt \frac{d\zeta}{dt} U_{\text{EAM}}, \quad (5)$$

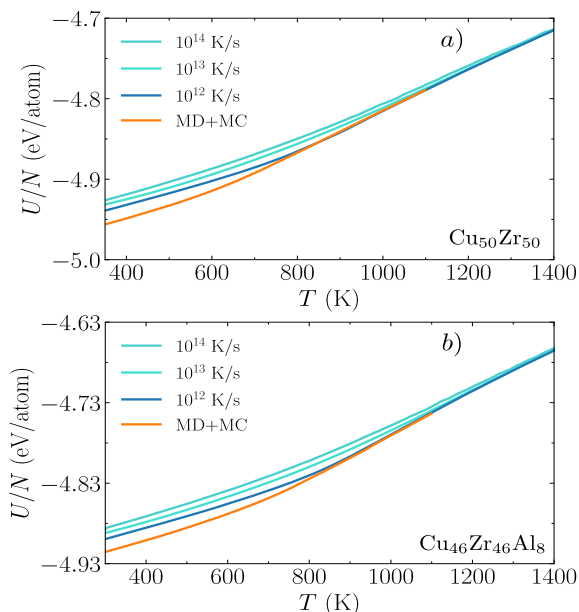


FIG. 7. Potential energy for various cooling rates for the MD vs. the hybrid algorithm for a) Zr-Cu and b) Zr-Al.

where T_0 is the temperature at which G_{EAM}^0 was estimated in item (ii) and t_{sim} is the simulation time.

- (iv) Finally, the configurational entropy is obtained as:

$$S_{\text{conf}} = S_l - S_g, \quad (6)$$

where S_l and S_g are the liquid and glass entropies, respectively.

The reference free energy G_{EAM}^0 in Eq. (3) is obtained by transforming the MEAM interaction into a reference system by means of AS method. For the solid phase at $T=300$ K, we used the Einstein crystal with a spring constant $\alpha=5eV/\text{\AA}^2$ for all the particles of the system[46, 64]. The liquid phase, on the other hand, G_{EAM}^0 was obtained at $T=2800$ K using as a reference the Uhlenbeck-Ford model (UFM) defined as[45, 65]:

$$U_{\text{UFM}}(r) = -\frac{p}{\beta} \ln \left(1 - e^{-(r/\sigma)^2} \right), \quad (7)$$

where $\beta=1/(k_B T)$ is the inverse of the temperature times the Boltzmann constant k_B , and p and σ are the softness and length scaling parameters, respectively. Following Paula-Leite et al.[45] a value of $p=50$ gives a liquid-like behavior for the UFM system. The quasistatic work W_{AS} is estimating and evaluating the irreversible work during two adiabatic switching trajectories. One transforming the system from the EAM to the reference system ($W_{\text{EAM} \rightarrow \text{ref}}^{\text{irr}}$) and the other one in the inverse process ($W_{\text{ref} \rightarrow \text{EAM}}^{\text{irr}}$). The irreversible work done in the AS method is calculated by $W^{\text{irr}} = \int_0^{t_{\text{sim}}} dt \frac{d\lambda}{dt} U(\Gamma_\alpha)$, where $U(\Gamma_\alpha)$ is the hybrid potential connecting U_{EAM} and U_{ref} and λ is the AS coupling parameter. Thus,

$$W_{\text{AS}} = \frac{1}{2} (W_{\text{EAM} \rightarrow \text{ref}}^{\text{irr}} - W_{\text{ref} \rightarrow \text{EAM}}^{\text{irr}}) \cdot a \quad (8)$$

Equation (8) is only valid if the dynamical work is performed slowly enough for holding the system in the linear response regime[44, 61].

In Fig. 8 we show the absolute values of the free energy and the entropy obtained by the RS method of the ternary $\text{Cu}_{46}\text{Zr}_{46}\text{Al}_8$.

- [1] A. L. Greer, Metallic glasses, *Science* **267**, 1947 (1995).
- [2] A. Inoue, Stabilization of metallic supercooled liquid and bulk amorphous alloys, *Acta Materialia* **48**, 279 (2000).
- [3] W.-H. Wang, C. Dong, and C. Shek, Bulk metallic glasses, *Materials Science and Engineering: R: Reports* **44**, 45 (2004).
- [4] M. Ashby and A. L. Greer, Metallic glasses as structural materials, *Scripta Materialia* **54**, 321 (2006).
- [5] J. Schroers, Processing of bulk metallic glass, *Advanced Materials* **22**, 1566 (2010).

[6] W. L. Johnson, Bulk glass-forming metallic alloys: Science and technology, *MRS bulletin* **24**, 42 (1999).

[7] H.-B. Yu, Y. Luo, and K. Samwer, Ultrastable metallic glass, *Advanced Materials* **25**, 5904 (2013).

[8] M. Lüttich, V. M. Giordano, S. Le Floch, E. Pineda, F. Zontone, Y. Luo, K. Samwer, and B. Ruta, Anti-aging in ultrastable metallic glasses, *Physical review letters* **120**, 135504 (2018).

[9] P. Luo, C. Cao, F. Zhu, Y. Lv, Y. Liu, P. Wen, H. Bai, G. Vaughan, M. Di Michiel, B. Ruta, *et al.*, Ultrastable metallic glasses formed on cold substrates, *Nature communications* **9**, 1389 (2018).

[10] Q. Sun, D. M. Miskovic, K. Laws, H. Kong, X. Geng, and M. Ferry, Transition towards ultrastable metallic glasses in zr-based thin films, *Applied Surface Science* **533**, 147453 (2020).

[11] Y. Zhao, B. Shang, B. Zhang, X. Tong, H. Ke, H. Bai, and W.-H. Wang, Ultrastable metallic glass by room temperature aging, *Science Advances* **8**, eabn3623 (2022).

[12] Q. Sun, D. M. Miskovic, and M. Ferry, Film thickness effect on formation of ultrastable metallic glasses, *Materials Today Physics* **18**, 100370 (2021).

[13] S. F. Swallen, K. L. Kearns, M. K. Mapes, Y. S. Kim, R. J. McMahon, M. D. Ediger, T. Wu, L. Yu, and S. Satija, Organic glasses with exceptional thermodynamic and kinetic stability, *Science* **315**, 353 (2007).

[14] K. L. Kearns, T. Still, G. Fytas, and M. Ediger, High-modulus organic glasses prepared by physical vapor deposition, *Advanced Materials* **1**, 39 (2009).

[15] I. Lyubimov, M. D. Ediger, and J. J. de Pablo, Model vapor-deposited glasses: Growth front and composition effects, *The Journal of Chemical Physics* **139** (2013).

[16] C. Rodriguez-Tinoco, M. Gonzalez-Silveira, M. A. Ramos, and J. Rodriguez-Viejo, Ultrastable glasses: new perspectives for an old problem, *La Rivista del Nuovo*

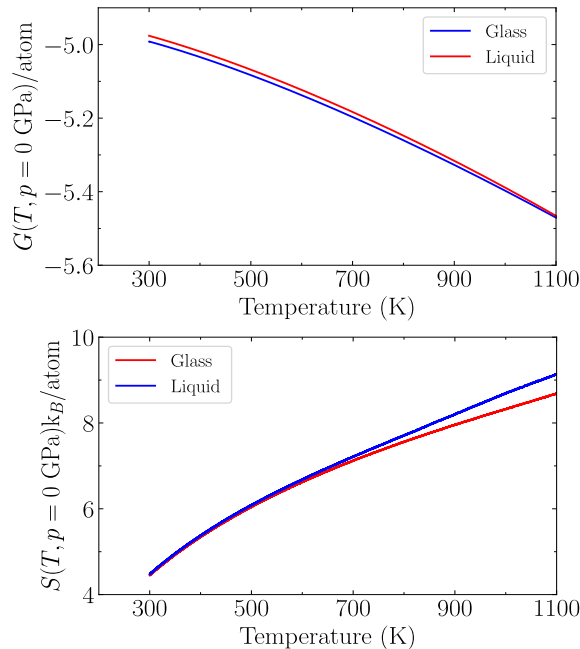


FIG. 8. Free energy and Entropy as a function of temperature obtained by the RS method of the ternary $\text{Cu}_{46}\text{Zr}_{46}\text{Al}_8$ alloy.

Cimento **45**, 325 (2022).

[17] P. G. Debenedetti and F. H. Stillinger, Supercooled liquids and the glass transition, *Nature* **410**, 259 (2001).

[18] J. C. Dyre, Colloquium: The glass transition and elastic models of glass-forming liquids, *Reviews of modern physics* **78**, 953 (2006).

[19] K. Binder and W. Kob, *Glassy materials and disordered solids: An introduction to their statistical mechanics* (World scientific, 2011).

[20] J. Ding, S. Patinet, M. L. Falk, Y. Cheng, and E. Ma, Soft spots and their structural signature in a metallic glass, *Proceedings of the National Academy of Sciences* **111**, 14052 (2014).

[21] J. Ashwin, E. Bouchbinder, and I. Procaccia, Cooling-rate dependence of the shear modulus of amorphous solids, *Physical Review E* **87**, 042310 (2013).

[22] R. Ryltsev, B. Klumov, N. Chtchelkatchev, and K. Y. Shunyaev, Cooling rate dependence of simulated $\text{Cu}_{64}\text{Zr}_{35.5}$ metallic glass structure, *The Journal of Chemical Physics* **145** (2016).

[23] Y. Zhang, F. Zhang, C. Wang, M. Mendeleev, M. Kramer, and K. Ho, Cooling rates dependence of medium-range order development in $\text{Cu}_{64}\text{Zr}_{35.5}$ metallic glass, *Physical Review B* **91**, 064105 (2015).

[24] K. Vollmayr, W. Kob, and K. Binder, How do the properties of a glass depend on the cooling rate? a computer simulation study of a lennard-jones system, *The Journal of Chemical Physics* **105**, 4714 (1996).

[25] Y. Liu, H. Bei, C. T. Liu, and E. P. George, Cooling-rate induced softening in a $\text{Zr}_{50}\text{Cu}_{50}$ bulk metallic glass, *Applied Physics Letters* **90** (2007).

[26] H. Yu, W. Wang, and H. Bai, An electronic structure perspective on glass-forming ability in metallic glasses, *Applied Physics Letters* **96** (2010).

[27] Y. Cheng, E. Ma, and H. Sheng, Atomic level structure in multicomponent bulk metallic glass, *Physical Review Letters* **102**, 245501 (2009).

[28] J. Ding and Y. Cheng, Charge transfer and atomic-level pressure in metallic glasses, *Applied Physics Letters* **104** (2014).

[29] S. Pauly, J. Das, N. Mattern, D. Kim, and J. Eckert, Phase formation and thermal stability in Cu-Zr-Ti (al) metallic glasses, *Intermetallics* **17**, 453 (2009).

[30] R. Gutiérrez, S. Karmakar, Y. G. Pollack, and I. Procaccia, The static lengthscale characterizing the glass transition at lower temperatures, *Europhysics Letters* **111**, 56009 (2015).

[31] L. Berthier, D. Coslovich, A. Ninarello, and M. Ozawa, Equilibrium sampling of hard spheres up to the jamming density and beyond, *Physical review letters* **116**, 238002 (2016).

[32] A. Ninarello, L. Berthier, and D. Coslovich, Models and algorithms for the next generation of glass transition studies, *Physical Review X* **7**, 021039 (2017).

[33] T. S. Grigera and G. Parisi, Fast monte carlo algorithm for supercooled soft spheres, *Physical Review E* **63**, 045102 (2001).

[34] L. Berthier, E. Flenner, C. J. Fullerton, C. Scalliet, and M. Singh, Efficient swap algorithms for molecular dynamics simulations of equilibrium supercooled liquids, *Journal of Statistical Mechanics: Theory and Experiment* **2019**, 064004 (2019).

[35] L. Berthier, P. Charbonneau, D. Coslovich, A. Ninarello, M. Ozawa, and S. Yaida, Configurational entropy mea-

- surements in extremely supercooled liquids that break the glass ceiling, *Proceedings of the National Academy of Sciences* **114**, 11356 (2017).
- [36] M. Ozawa, G. Parisi, and L. Berthier, Configurational entropy of polydisperse supercooled liquids, *The Journal of Chemical Physics* **149** (2018).
- [37] L. Berthier, M. Ozawa, and C. Scalliet, Configurational entropy of glass-forming liquids, *The Journal of Chemical Physics* **150** (2019).
- [38] A. D. Parmar, M. Ozawa, and L. Berthier, Ultrastable metallic glasses in silico, *Physical Review Letters* **125**, 085505 (2020).
- [39] B. Sadigh, P. Erhart, A. Stukowski, A. Caro, E. Martinez, and L. Zepeda-Ruiz, Scalable parallel monte carlo algorithm for atomistic simulations of precipitation in alloys, *Physical Review B* **85**, 184203 (2012).
- [40] M. S. Daw and M. I. Baskes, Embedded-atom method: Derivation and application to impurities, surfaces, and other defects in metals, *Physical Review B* **29**, 6443 (1984).
- [41] Z. Zhang, J. Ding, and E. Ma, Shear transformations in metallic glasses without excessive and predefinable defects, *Proceedings of the National Academy of Sciences* **119**, e2213941119 (2022).
- [42] S. Plimpton, P. Crozier, and A. Thompson, Lammgs-large-scale atomic/molecular massively parallel simulator, *Sandia National Laboratories* **18**, 43 (2007).
- [43] R. Alvarez-Donado, S. Cahahuaringa, and A. Antonelli, Revisiting the fragile-to-strong crossover in metallic glass-forming liquids: Application to $\text{Cu}_x\text{Zr}_x\text{Al}_{100-2x}$ alloy, *Physical Review Materials* **3**, 085601 (2019).
- [44] M. de Koning, A. Antonelli, and S. Yip, Optimized free-energy evaluation using a single reversible-scaling simulation, *Physical Review Letters* **83**, 3973 (1999).
- [45] R. Paula Leite, R. Freitas, R. Azevedo, and M. de Koning, The uhlenbeck-ford model: Exact virial coefficients and application as a reference system in fluid-phase free-energy calculations, *The Journal of Chemical Physics* **145** (2016).
- [46] R. Freitas, M. Asta, and M. De Koning, Nonequilibrium free-energy calculation of solids using lammgs, *Computational Materials Science* **112**, 333 (2016).
- [47] R. P. Leite and M. de Koning, Nonequilibrium free-energy calculations of fluids using lammgs, *Computational Materials Science* **159**, 316 (2019).
- [48] H. L. Smith, C. W. Li, A. Hoff, G. R. Garrett, D. S. Kim, F. C. Yang, M. S. Lucas, T. Swan-Wood, J. Y. Lin, M. B. Stone, *et al.*, Separating the configurational and vibrational entropy contributions in metallic glasses, *Nature Physics* **13**, 900 (2017).
- [49] K. Dawson, L. Zhu, L. A. Kopff, R. J. McMahon, L. Yu, and M. Ediger, Highly stable vapor-deposited glasses of four tris-naphthylbenzene isomers, *The Journal of Physical Chemistry Letters* **2**, 2683 (2011).
- [50] S. L. L. Ramos, M. Oguni, K. Ishii, and H. Nakayama, Character of devitrification, viewed from enthalpic paths, of the vapor-deposited ethylbenzene glasses, *The Journal of Physical Chemistry B* **115**, 14327 (2011).
- [51] C. E. Maloney and A. Lemaitre, Amorphous systems in athermal, quasistatic shear, *Physical Review E* **74**, 016118 (2006).
- [52] A. D. Parmar, B. Guiselin, and L. Berthier, Stable glassy configurations of the kob-andersen model using swap monte carlo, *The Journal of Chemical Physics* **153**, 134505 (2020).
- [53] E. Bitzek, P. Koskinen, F. Gähler, M. Moseler, and P. Gumbsch, Structural relaxation made simple, *Physical review letters* **97**, 170201 (2006).
- [54] T. L. Cheung and S. C. H, Thermal and mechanical properties of cu-zr-al bulk metallic glasses, *Journal of Alloys and Compou434-435* **434-435**, 71.
- [55] J. Zhang, Z. Zhou, Z. Zhang, M. Park, Q. Yu, Z. Li, J. Ma, A. Wang, H. Huang, M. Song, *et al.*, Recent development of chemically complex metallic glasses: from accelerated compositional design, additive manufacturing to novel applications, *Materials Futures* **1**, 012001 (2022).
- [56] S. Bonfanti, R. Guerra, R. Alvarez-Donado, P. Sobkowicz, S. Zapperi, and M. Alava, Quasi-localized modes in crystalline high entropy alloys, *arXiv preprint arXiv:2303.09161* (2023).
- [57] B. Guiselin, C. Scalliet, and L. Berthier, Microscopic origin of excess wings in relaxation spectra of supercooled liquids, *Nature Physics* **18**, 468 (2022).
- [58] J. M. Rickman and R. LeSar, Free-energy calculations in materials research, *Annual Review of Materials Research* **32**, 195 (2002).
- [59] M. Watanabe and W. P. Reinhardt, *Phys. Rev. Lett.* **65**, 3301 (1990).
- [60] M. de Koning and A. Antonelli, *Phys. Rev. B* **55**, 735 (1997).
- [61] M. de Koning, A. Antonelli, and S. Yip, *J. Chem. Phys.* **115**, 11025 (2001).
- [62] C. R. Miranda and A. Antonelli, *J. Chem. Phys.* **120**, 11672 (2004).
- [63] J. G. Kirkwood, *J. Chem. Phys.* **3**, 300 (1935).
- [64] D. Frenkel and A. J. Ladd, *The Journal of chemical physics* **81**, 3188 (1984).
- [65] R. Paula Leite, P. A. Santos-Flórez, and M. de Koning, *Phys. Rev. E* **96**, 032115 (2017).